Original Article

Use of Remote Sensing Data in Comprehending an Extremely Unusual Flooding Event over Southwest Bangladesh

Ehsan H. Chowdhury[1,2], Quazi K. Hassan[1]

[1]Department of Geomatics Engineering, Schulich School of Engineering, University of Calgary, 2500 University Dr NW, Calgary, Alberta T2N 1N4, Canada

[2]Center for Environmental and Geographic Information Services (CEGIS), House # 6, Road # 23/C, Gulshan 1, Dhaka 1212, Bangladesh

Abstract

Flooding is one of the natural disasters that affect the livelihood of the people living in the floodplains, like Bangladesh. Here, we proposed to employ SAR satellite images in assessing the flood extent and crop damage with the hydro-meteorological observations in the southwestern region of Bangladesh. We observed that the unusual flood of the year 2000 was the combined effect of the huge amount of rainfall in the local areas as well as oncoming water flows from West Bengal in India. During late monsoon of 2000, we experienced that the amount of rainfall was in several magnitudes (250-450 %) than the expected over the region. Bangladesh, one of the largest delta in world in general experience recurrent flood events from the spill of the three mighty rivers in every year. However, we observed that during 2000 the river situation was slightly above the average year conditions and below the moderate level of flood warning conditions, indicating non riverine flooding. Therefore, we used the SAR images in delineating the flood extent and its damages for the standing *aman* crops. We observed that the flood extent mapping was having more than 95 % agreements with the ground data; and crop damage information was about 75 % in agreement with the government estimates. The flood extent and crop damage map was found to be useful during the unprecedented flood in the southwestern region of Bangladesh. The use of near realtime SAR imageries thus would be helpful in developing strategies for flood management and disaster mitigation activities; and could be utilized on a regular basis.

Keywords: flood extent, flood damage, rainfall, water level, RADARSAT

1 Introduction

Flooding is one of the most devastating natural hazards/disasters that account for approximately 40 % of all sorts of natural disasters across the world (Bach et al. 2011). In Bangladeshi context (i.e., a country lying mostly at the bottom of the flood plains of three large rivers, namely the Ganges, the Brahmaputra and the Meghna), it extensively suffers from the monsoon flooding during mid June to mid-September every year. In fact, one or more of the following factors can potentially cause flooding, such as: (i) upstream contributions that include rainfall in the upper catchment areas of these rivers in India and Nepal that contributes approximately 92.5 % of the total flow, and snow melting in the Himalayas (NWMP 2001; Mirza 2011); (ii) local rainfall (Dewan et al. 2003); and (iii) slow down of the water discharge to the Bay of Bengal as the wind direction (i.e., from south towards north) opposes the overall direction of the water flow (i.e., north to south or northwest to southeast) (Narvekar and Prasanna 2014). In general, these flooding events largely influence the livelihood of the people living in the floodplains. For example, Bangladesh experienced inundation with more than 60 % of the country with severe destruction and damage to households, standing crops, livestock, and infrastructures during the extreme flooding events in 1988, 1998, 2004, 2007, and 2014 (IPCC 2007; Ghatak et al. 2012; Dewan 2015; Rashid and Pramanik 1993) in particular. On the contrary, a period of 'lean' flooding adversely affects freshwater fishery resources and forces the farmers to irrigate the crops from alternate sources. Furthermore, the timing of the onset of flooding, its peak and recession often determine not only the planting time of the dominant monsoon rice crop (known as *aman* rice) but also the variety of *aman* to be planted and their respective yield. In general, two types of aman crop grow in Bangladesh i.e., broadcast and transplant *aman,* which account approximately 38.9 % of the total rice production (BBS 2015). The broadcast *aman* are sown during April/May in low lands (seasonal flood inundation over 180 cm), and transplant *aman* are planted during late June/July in medium high to high lands (seasonal flood inundation not more than 90 cm); and both of the *aman* types are harvested during November/December (Rahman et al. 2012; MPO 1987; Bhuiyan et al. 2004).

In order to comprehend and develop management strategies, we must have flood monitoring mechanism in place. In this context, Bangladeshi National Agencies such as the Flood Forecasting and Warning Centre (FFWC), Bangladesh Water Development Board (BWDB), and Bangladesh Meteorological Department (BMD), regularly measure hydrological and meteorological conditions (i.e., river discharge/water level and rainfall in particular) at selected sites. Then, FFWC employs mathematical models in order to generate potential flooding scenarios intent to distribute among the various stakeholders. In general, these models require detailed information about watershed characteristics derived from digital elevation model, land use/land cover map from ground/satellite data, and soil characteristics. In addition, point-based measurements of water level and discharge, temperature, relative humidity, wind speed and direction, and precipitation regimes are also required. Thus, acquisition of these data in near real time-basis are not only challenging but also quite expensive and labour intensive. In addition, the gauge stations are often displaced during the severe flooding events. One of the alternate data sources could be the use of satellite-based remote sensing data/imagery, which has been employed successfully in comprehending flooding monitoring purposes (Veiga et al. 2016; Bach et al. 2005; Yilmaz et al. 2010; Wu et al. 2014). This is the case as remote sensing platforms are capable of acquiring images of the earth's surface at a regular intervals, thus provides an enormous opportunity to monitor the dynamics at both landscape and temporal scale (NRCAN 2016; Hoque et al. 2011; Bhatt and Rao 2016).

In case of remote sensing, there are two broad types of platforms, such as optical and radar remote sensing. For optical platforms, they acquire the surface reflectance regimes over the visible (i.e., 0.4-0.7 μm) and short wave infrared (i.e., 0.7-2.5 μm) spectral bands; and use to define flooding extent maps (Klemas 2014; Lamovec et al. 2013; Qi et al. 2009). However, these satellites depends on the sunlight to illuminate the earth surface and unable to view the earth surface under cloudy sky conditions, which is often a dominant factor during the flooding time period. For example, Veiga et al. (2016) found that the Landsat ETM+ optical sensor acquired an image on 20 June 2013, that coincided with the peak of the 2013 devastating flooding over the Bow River Basin in Calgary, Alberta, Canada. Despite, the image was completely useless as it was unable to depict the flooding dynamics due to extremely heavy cloudy sky. On the contrary, the radar platforms (in particular to the active ones) are capable of imaging during both day or night (i.e., independent from the sun as an illumination source), and under any weather conditions (e.g., haze, light rain, snow, clouds, or smoke) (Nirupama and Simonović 2002; Bates 2012). Some of the examples of flood extent estimation using radar images are worthwhile to describe briefly. For example, Kiage et al. (2005) employed multi-temporal RADARSAT-1 SAR images to detect flooded areas in coastal Louisiana after Hurricane Lili. Mason et al. (2012) used TerraSAR-X to detect flooded areas around Tewkesbury, U.K, by calculating an average intensity-based optimal threshold that would segregate water/flooded objects from the non-flooded ones. Brivio et al. (2002) used two ERS-1 SAR images, i.e., one collected one month before and the second one was just after the 3 days of the flooding event that occurred in 1994 over Regione Piemonte, Italy. In this case, they employed both visual interpretation and two different thresholding techniques in order to derive a flooding extent map.

During the late September of 2000 (i.e., that fell beyond the normal time of flooding period), an extremely unusual disastrous flooding event took place in the southwest region of Bangladesh. In fact, late monsoon rainfall within the catchments of the river basins in neighboring India triggered this event, which created catastrophic damages to the standing crops and livelihood of the people living in the floodplains in the downstream reaches within Bangladesh. Thus, the overall objective of the study was to comprehend the dynamics of these particular flooding event primarily using radar remote sensing data such as RADARSAT ScanSAR multi-temporal images. The specific objectives were to analyse the: (i) impact of local rainfall (i.e., within the study area; see Fig. 1) in this particular event using ground-based precipitation data; (ii) contribution of upstream via interpreting the water levels at several key sites in the major rivers that constitute the study area (see Fig. 1); and (iii) extent and damage of the flooding in the context of agriculture crop and settelement using RADARSAT ScanSAR multi-temporal images.

Figure 1

2 Study Area and Data Requirements

2.1 Study area

In this study, we considered the southwest region of Bangladesh that included the flood affected districts of Meherpur, Chuadanga, Jhenidah, Jessore, and Satkhira (see Fig. 1 for their geographical extents). This particular region is, in fact, one of the least flood vulnerable areas in Bangladesh. However, the region observed an extremely unusual flooding event during late monsoon, i.e., after 15 September of 2000. It primarily happened as a result of the huge amount of rainfall during the days between 18-22 September 2000 in some districts of the Indian State of

West Bengal and Bangladesh. In India, the districts included Birbhum (1575 mm), Murshidabad (1201 mm), and Nadia (1232 mm) in particular (Chakraborty and Chakraborty 2011); where the regional annual average rainfall of the region (i.e., known as Gangetic West Bengal) was approximately 1439 mm (available from http://www.rainwaterharvesting.org/urban/rainfall.htm accessed on 19 May 2016). Consequently, the Mayurakhshi, Pagla, Pasloi, Brakkhani and Bhagirati basins in West Bengal were flooded and then water entered into Bangladesh. In addition, the Mayurakshi and Damodar reservoirs of West Bengal, filled with water during the monsoon, were also released (Chakraborty and Chakraborty 2011). Under these circumstances, a huge amount of floodwater spilled into the Kumar-Nabaganga, Begabati-Bhadra and Kobadak system. The overflowing of the rivers Kodla and Ichhamoti; and the contribution of local rainfall in the study area caused flooding in the districts of Meherpur, Chuadanga, Jhenaidah, Jessore and Satkhira in the southwest region of Bangladesh.

2.2 Data

Here, we acquired daily rainfall data available from the Water Resources Planning Organization over the period 1965-2010 at 4 stations (i.e., Kushtia, Jessore, Khulna, and Satkhira). We then calculated rainfall normals at decadal (i.e., accumulation of 10 days) scale using the long-term data; and subsequently compared with the 2000 rainfall regimes in order to determine its deviations. We also obtained water level data at 3 sites (i.e., Hardinge Bridge on the Upper Ganges River, Gorai Railway Bridge on the Gorai River, and Insafnager on the Mathabanga River) during the period 1965-2010. We used the time series data to define the site-specific "*danger level*" (i.e., defined as the water level that might potentially cause damage to crops and homesteads). In a river without embankments, the danger level would be determined on the basis of the annual average flood level. In an embanked river, the danger level would be calculated slightly below the designed flood level of the embankment (FFWC, 1998). In these cases, equal or greater water level than the *danger level* would initiate the process of inundating and/or damaging the settlements and agriculture crops in the surrounding areas.

We also acquired five RADARSAT SAR ScanSAR Wide (SWB) images having a spatial resolution of 50 m during the monsoon and late monsoon season of 2000 (see Table 1 for details). In addition, we also employed an internet preview image of IRS LISS (having a spatial resolution of 24 m) acquired over the southwest of Bangladesh on 14 October 2000. In case of the SAR image acquired on 28 September 2000, we used it to comprehend that huge amount of water spilled from West Bengal, India and caused the devastating flooding over the southwest region of Bangladesh. In addition, we used the IRS LISS image acquired on 14 October 2000 to delineate the flood damages.

Table 1

In addition to the remote sensing data as described above, we conducted an extensive ground thruthing on 24-26 October 2000 over the flooded area in the southwest region of Bangladesh aided by high resolution remote sensing images and GPS receivers. During collection of ground truthing data; we recorded the coordinates of the locations, took photographs and made visual inspection of the area of interest, investigated the water marks in the large trees and settlements for each block (i.e., areas dependent on the same resources). Furthermore, we consulted with the local people and recorded the field information regarding flood extent, submergence/damages of standing crop (i.e., *aman*), and settlements in detail at 26 sites across the study area. We also gathered a general overview of the landuse/landcover over approximately 3 % of the area of the flood affected districts on an average. Figure 1 shows the locations of these field polygons on top of the Landsat TM images of 1997. In addition, we also obtained crop (in particular to *aman*) damage information at sub-district (also known as Thana)-level from the Department of Agricultural Extension (DAE) under the Ministry of Agriculture (MoA) of Bangladesh.

3 Methods

3.1 Processing of hydro-meteorological data

We processed the historical time series of rainfall and water level data at daily and decadal (i.e., 10 day accumulation) scales in view to understand the hydro-meteorological conditions of the year 2000 and their settings with the prevailing warning systems/ danger conditions. In general, authorities would issue rainfall warnings when the daily total amount of rainfall would exceed 50 mm (FFWC 2012; EC 2016) or decadal total rainfall would exceed 300 mm (FFWC 2012). So thus, we analyzed the year 2000 rainfall data to find the following conditions: (i) generation of daily and decadal amount of rainfall to understand the local drainage congestion/ flooding pattern; and (ii) comparison with respect to different excedence probabilities (i.e., 10, 50, and 90 % of the time, respectively). Upon analyzing the rainfall data, we investigated each of the individual stations with respect to the above conditions.

In case of water level, we investigated the setting of water levels with respect to danger levels and calculated the probable values at different frequencies (10, 50, and 90 % of the time); and their relationship with the flood conditions. In Bangladesh, according to the setting of river water levels, three categories of floods were presented (e.g., normal, moderate, and severe flood depending on the river water level below 50 cm of the danger level; 50 cm above danger level;

and beyond 50 cm above the danger level, respectively). In this study, we examined the setting of the year 2000 water levels at some key stations to demonstrate the categories of flooding in our region of interest. Note that we used *Extreme Value Distribution (EVD) Type I* to calculate the probable values in both rainfall and water level analysis. The *EVD Type I* distribution has the following probability density function:

$$f(x) = \frac{1}{\boldsymbol{\sigma}}\exp(-z - \exp(-z)) \tag{1}$$

where, z = (x - μ)/σ, x is the decadal values of the variable of interest, μ is the location parameter, and σ is the distribution scale (σ>0).

3.2 Processing of satellite data

We co-registered three RADARSAT ScanSAR images (acquired on 13 Aug., 06 Sep., and 30 Sep. 2000 in ascending mode) with respect to each other. Note that we were unable to co-register the image acquired on 25 Oct. 2000, which was captured in descending mode that differed from images. We performed the co-registration through necessary shifting of the images in the X and Y direction as described in Hassan et al. (2003). We did the shifting of each image with respect to one reference image using a stable high backscattering feature. As this operation did not involve re-sampling of the data, we were able to retain the original data values for further analysis. Upon co-registration, we found that the registration errors were within one pixel in both X and Y directions. After the co-registration, we applied a 3x3 Gamma-Map filter over all the RADARSAT images, including the descending mode RADARSAT image in order to reduce the speckles as implemented in other studies, such as: (i) Senthilnath et al. (2013) investigated three filtering methods (i.e., Lee, Frost, and Gamma Map) for extracting the flood extent area over

Bihar of India, and found the Gamma-Map was the best one; (ii) Long et al. (2014) used the Gamma-Map for mapping the flood extent over the Chobe floodplain of Namibia; and (iii) Hassan and Bourque (2015) employed Gamma-Map for developing a wetness index over forested areas of New Brunswick, Canada. We then georeferenced the filtered RADARSAT images using Landsat TM mosaic image of 1997 as a reference one. It would be worthwhile to mention that we found the accuracy of georeferencing within in a pixel (i.e. ± 50 m).

Upon generating a multi-temporal data set consisting of all the four RADARSAT images, we performed an unsupervised classification called ISODATA clustering technique (Lillesand and Kiefer 2000) in order to generate 100 classes. In this case, we set a convergence threshold equal to 0.995 with unlimited iterations like other studies (e.g., Mosleh and Hassan 2014), where the goal was to end the process upon achieving the convergence threshold. We then analysed the class-specific signatures by use of ground truthing and IRS LISS data; and grouped them into seven broad classes. Those included: (i) flooded settlements, (ii) water (except on 25 Oct.), (iii) water on all dates, (iv) survived *aman*, (v) moderately damaged *aman,* (vi) severely damaged *aman*, and (vii) others not affected by flooding. We then compared the RADASAT-derived damaged *aman* (that included both moderate and severely ones) areas against the DAE estimates at sub-district level.

4 Results and Discussion

4.1 Impact of local rainfall regimes on the flooding event

Figure 2 shows the daily and decadal total rainfall characteristics for the four selected stations with respect to their settings with local warning conditions, i.e., daily rainfall of 50 mm and 10-day cumulative rainfall of 300 mm, respectively. It was evident from the figure that during late

September, the study area observed heavy rainfall (i.e., more than 100 mm at daily scales in all four stations) which might create local flooding. Furthermore, the cumulative 10-day total rainfall was also exceeded 300 mm threshold value indicating local drainage congestions/ flooding that added to the oncoming overland flow from the upper catchments from West Bengal of India. We observed that these rainfall amounts observed within our area of interests were more than the average year conditions (i.e., 50 % of the time) in the scale of 250-450 % during late September (see Table 2 for details).

Figure 2

Table 2

In addition, we compared the decadal total rainfall distribution with different probabilities (i.e., 10, 50, and 90 %) (see Fig. 3). It was evident from the figure that in all four selected stations, the total amount of rainfall crossed the 10 % of the time (i.e., 1 in 10 year return period) during late September. So, this high amount of rainfall distribution had a huge impact on local flooding in addition to the extreme rainfall events in the upper catchment in India (see study area and data description section).

Figure 3

4.2 Contribution of upstream water levels/flow on the flooding event

To understand the river situations during year 2000 and causes of flooding, we compared the three river stations (i.e., Hardinge Bridge at Ganges River, Gorai Railway Bridge at Gorai River, and Insafnagar at Mathabanga River) with the danger levels. Figure 4 showed that all the upper catchment rivers of the study area within the Bangladesh were flown below the danger levels during the peak flooding periods; and set up below moderate level flooding. So thus, we might concluded that the riverine water flows didn't cause this unusual flooding in the southwest region of Bangladesh, rather accumulation of overland flow of rainfall from the upper catchments of India and contributions of local rainfall in the region. Furthermore, we opted to investigate the extent and damage of flooding using remote sensing-based imageries as described in the subsequent sections.

Figure 4

4.3 Extent and damage of the flooding

As mentioned, the southwest region of Bangladesh was not affected by flood over a long time period. The region was in fact remained flood-free even during the devastating floods of 1988 and 1998 as illustrated in Fig. 5. The dark areas show the open water flooding extent in the month August during 1998 and 2000, where August would be normally the month for the largest flooding in Bangladesh. It was apparent that even during the period of peak flooding, the southwest region (blue box in the images) remained unaffected by devastating flooding event in both 1998 and 2000.

Figure 5

As described earlier that this particular flooding event was a result of excessive rainfall in the adjacent Indian State of West Bengal and southwestern region of Bangladesh, thus we opted to comprehend through RADARSAT images as well. In this context, we extracted the extent of open water (as shown in blue color) from two RADARSAT images acquired on 28 Sep. 2000 and 30 Sep. 2000 over portion of West Bengal, India and southwest of Bangladesh, respectively (see Fig. 6 for details). In extracting such extent of open water, we classified the individual images separately using density slicing techniques (Knight et al. 2009; Jain et al. 2005). We observed that the low valued pixels (i.e., the darker pixels) represented the open water category (as seen in blue color in Fig. 5). Finally, it was evident that the floodwater entered from West Bengal towards the southwest region of Bangladesh as this flooding event was unrelated with compare to upstream river conditions.

Figure 7 shows the extracted signature patterns for the 7 classes (see Section 3.2). We found that the backscatterings for the water (all times) class were almost similar in all dates (13 Aug. - 25 Oct.). In case of water (except 25 Oct.) class, the backscatterings were less in earlier three dates (13 Aug. - 30 Sep.) and high in late October as due to water drainage. The damaged *aman* classes (i.e., both moderately and severely damaged) were under water/inundated during 30 Sept., where the moderately damaged *aman* showed higher backscatterings compared to severely damaged *aman*. Moreover, the backscattering signature of the survived *aman* was increasing trend over the entire growth stages. In case of flooded settlements, the backscattering was relatively similar except on 30 Sept. Furthermore, we verified the classified images (i.e., flood extent and aman damaged area) with the ground truthing data for accuracy assessment (see Table 3 for details). Here, we observed overall accuracy and kappa coefficients 84 % and 0.80, respectively. Our findings were similar to other studies found in the literature, such as (i) Asare-Kyei et al. (2015) utilized GIS and remote sensing imageries (i.e., RapidEye, TerraSAR-X images) to delineate the flood hazard zones over several communities in West Africa; and found overall accuracies in the range 88 - 97 %; and (ii) Kudahetty (2012) used ASAR IM images to derive the open water, flooded, non-flooded, and urban areas over Kelani Ganga and Bolgoda basins of Sri Lanka; and observed overall accuracy and kappa coefficients of 88.35 % and 0.84, respectively.

Figure 6

Figure 7

Table 3

Figure 8 shows flood damage map generated solely by use of four RADARSAT ScanSAR images acquired on 13 Aug., 6 Sep., 30 Sep., and 25 Oct. 2000. In this case, we also used ground thruthing and an IRS LISS image as auxiliary data sources. Our analyses demonstrated that the Maheshpur (i.e., 24,668 ha) and Sarsa (i.e., 23,903 ha) sub-districts were most severely affected by flood waters, followed by Damurhuda (i.e., 13,619 ha), Meherpur Sadar (i.e., 11,465 ha), Chaugacha (i.e., 9,875 ha), Jhikargachha (i.e., 8,791 ha), and Satkhira Sadar (i.e., 8,745 ha) sub-districts. The other sub-districts (that included Jibannagar, Kalaroa, Gangni, Tala, and Debhata) in the region were moderately flooded with an area less than 7,050 ha. We then compared these estimates with the ground-based estimates performed by Department of Agriculture, Bangladesh (see Fig. 9 for more details); and found reasonably good agreements (i.e., $r^2 \approx 0.75$ with a slope of 0.87 and an intercept of 139.65 ha for the regression equation). We obtained fairly good agreement (i.e., within ± 25 % of the ground-based estimates) for the sub-districts of Maheshpur, Sarsa, Damurhuda, Jhikargachha, Sathkira Sdara, Jibannagar, and Tala and Damurhuda. On the other hand, a few mismatches also appeared in the case of the sub-districts of Meherpur Sadar, Gangi, and Chaugacha. The rationales behind these discrepancies might be related with one or more of the following reasons, such as: (i) the spatial resolution of the RADARSAT images were moderate (i.e., 50 m x 50 m), thus it wouldn't be possible to delineate *aman* fields smaller than 2500 m^2 in size; (ii) drainage patterns for these sub-districts were better so that they discharged logged water within a time period that would still be reasonably fine for the survival of the crop; and (iii) DAE synthesised the ground-based damage estimates upon concluding the entire *aman* growing season (i.e., mid to late November); however, we acquired our fourth RADARSAT image on 25 Oct. that was unable to capture the complete dynamics of the *aman* damage.

Figure 8

Figure 9

In general, the southwest region of Bangladesh had become a poorly drained area over the time. For example, since the Farakka dam's construction in the Indian State of West Bengal in the 1970's, it has been often used to withdraw water in the dry season in particular, which caused reduced fresh water flow into the Betna and Kobadak river system (i.e., the major drainage and waterways in the southwest of Bangladesh). Such reduction in the flow caused heavy siltation in the upper stream of Betna and Kobadak. In addition, Bangladesh had constructed polders (i.e., artificial enclosures to protect lands from the saline water intrusion) in the coastal areas that created morphological changes and reduced the tidal effects. Also, public encroachment (i.e., shrimp *ghers* and other fish farms, roads and embankment construction) on the routes of the natural drainage system also disrupted floodwater drainage. Due to reduction of tidal effects and low flow of water in dry seasons, a heavy siltation occurred near the mouth of the sluice gates rendering them useless. The high tide in the Bay of Bengal also prevented the water from draining into the Bay of Bengal. In order to save the shrimp *ghers*, shrimp farmers put obstructions in the path of the floodwater flowing downstream. Due to these reasons the floodwater could not drain out rapidly and caused massive damage to crops, settlements and road network (FFWC 1998; Hossain 2000).

5 Conclusions

In this paper, we attempted to delineate the flood extent and assess the damage of the *aman* crop using RADARSAT images with hydrometeorological observations which might be useful in monitoring recurrent flood events in Bangladesh. Here, we compared the year 2000 rainfall situation with the average year conditions and observed highest (i.e., 250-450 %) during late September. It revealed that the daily rainfall was higher than 50 mm in three to five occurrences in all the four stations. The decadal rainfall was also been observed over 300 mm in several occasions. In addition to the local rainfall, the incoming water from India flows through the southwestern region of Bangladesh and created heavy damages to the standing *aman* crops. This observation connects well with the image acquired during late September 2000. In general, Bangladesh (e.g., one of the largest delta in the world) experienced recurrent flooding from overbank flows of the major rivers in almost every year. However, the water level situation in the major rivers during 2000 showed that all rivers flown below the moderate flood levels, and slightly above the average year conditions (i.e., 50 % of the time) indicating non-riverine flooding in the southwestern region. Thus, in comprehending the flood extent and damages of the *aman* crop in the flood affected areas, we found that the use of RADARSAT images would provide effective base information for mapping, monitoring, and assessment of damages. While comparing the damage assessment with the ground-based estimates; we found reasonably good agreements (i.e., $r^2 \approx 0.75$). Thus, the study provided a good overview of the flood extent mapping, damage assessment, and might help relevant agencies to plan rehabilitation programs in a timely manner.

Acknowledgements

We acknowledge the funding support by The Netherlands Government through the Ministry of Water Resources, Government of Bangladesh. We are thankful to RADARSAT Canada for providing the SAR images. We also oblige to Center for Environmental and Geogrphical Information Services, Water Resources Planning Organization, and Department of Agricultural Extension for providing hydro-meteorological and agricultural damage information at free of cost. We would like to acknowledge the anonymous reviewers for their comments.

References

Asare-Kyei D, Forkuor G, Venus V (2015) Modeling flood hazard zones at the sub-district level with the regional model integardted with GIS and remote sensing approaches. Water 7:3531-3564 doi:10.3390/w7073531

Bach H, Appel F, Fellah K, de Fraipont P (2005) Application of flood monitoring from satellite for insurances, Proceedings of IEEE Int GeoSci Remote Sens Symp. IGARSS 2005, 4p

Bates PD (2012) Integrating remote sensing data with flood inundation models: how far have we got? Hydrol Process 26(16):2515–2521

BBS (Bangladesh Bureau of Statistics) (2015) Estimate of major crops 2015-2016. Bangladesh Bureau of Statistics, Government of the People's Republic of Bangladesh, Web: http://www.bbs.gov.bd/PageWebMenuContent.aspx?MenuKey=241. Accessed on 1 November 2016

Bhatt CM, Rao GS (2016) Ganga floods of 2010 in Uttar Pradesh, north India: a perspective analysis using satellite remote sensing data, Geomatics. Nat Hazards and Risk 7(2):747-763. doi: 10.1080/19475705.2014.949877

Bhuiyan SI, Abedin MZ, Singh VP, Hardy B, editors. (2004) Rice research and development in the flood-prone ecosystem. Proceedings of the international workshop on flood-prone rice systems held in Gazipur, Bangladesh, 9-11 January 2001. Los Baños (Philippines): International Rice Research Institute, 283p

Bich TH, Quang LN, Thanh Ha LT, Duc Hanh TT, Guha-Sapi, D (2011) Impacts of flood on health: epidemiologic evidence from Hanoi, Vietnam. Global Health Action 4. doi: 10.3402/gha.v4i0.6356.

Brivio PA, Colombo R, Maggi M, Tomasoni R (2002) Integration of remote sensing data and GIS for accurate mapping of flooded areas. Int J Remote Sens 23(3):429–441

Chakraborty PK, Chakraborty S (2011) A hydro meteorological study of a most devastating flood in Gangetic West Bengal in September 2000. Mausam 64(2):371-384

Dewan AM, Makoto N, Mitsuru K (2003) Floods in Bangladesh: A comparative hydrological investigation on two catastrophic events. J F Environ Sci Tech. Okayama University 8(1):55-62.

Dewan TH (2015) Societal impacts and vulnerability to floods in Bangladesh and Nepal. Weather and Climate Extremes 7(2015):36-42

EC (Environment Canada) (2016) Public alerting criteria, website: http:// http://www.ec.gc.ca/meteo-weather/default.asp?lang=En&n=d9553ab5-1, Accessed 17 June 2016

FFWC (Flood Forecasting and Warning Center) (1998) Monthly Flood Report, Flood Forecasting & Warning Center, Processing and Flood Forecasting Circle, Hydrology, Bangladesh Water Development Board, September, Dhaka

FFWC (Flood Forecasting and Warning Center) (2012) Annual flood report, website: http://ffwc.gov.bd/index.php/reports/annual-flood-reports, Accessed 17 June 2016

Ghatak M, Kamal A, Mishra OP (2012) Background paper flood risk management in South Asia. In: Proceedings of the SAARC Workshop on Flood Risk Management in South Asia

Hasan K, Hassan QK, Huque I (2003) Mapping the monsoon landuse/landcover in Bangladesh using RARDSAT-1 and ERS-2 images: a comparative study. Proceedings of ASPRS Annual Conference, 9p (on CDROM)

Hassan QK, Bourque CPA (2015) Development of a new wetness index based on RADARSAT-1 ScanSAR data. In J. Li and X, Yang (eds.), Monitoring and Modeling of Global Changes: A Geomatics Perspective, Switzerland: Springer International Publishing, pp. 301-314

Hoque R, Nakayama D, Matsuyama H, Matsumoto J (2011) Flood monitoring, mapping and assessing capabilities using RADARSAT remote sensing, GIS and ground data of Bangladesh. Nat Hazards 57(2):525-548

Hossain ANHA (2000) Late Monsoon Flood in the Southwest Region of Bangladesh 2000, Paper presented in a seminar organized by Civil Engineering Division IEB, Dhaka.

IPCC (Intergovernmental Panel on Climate Change) (2007) Contribution of Working Group II to the Fourth Assessment Report of the Intergovernmental Panel on Climate Change. In: Parry, M.L., Canziani, O.F., Palutikof, J.P., van der Linden, P.J., Hanson, C.E. (Eds.) Cambridge University Press, Cambridge, United Kingdom and New York, NY, USA

Jain SK, Singh RD, Jain MK, Lohani AK (2005) Delineation of flood-prone areas using remote sensing techniques, Water Resour Manage 19: 333–347. DOI: 10.1007/s11269-005-3281-5

Kiage LM, Walker ND, Balasubramanian S, Babin A, Barras J (2005) Applications of Radarsat- 1 synthetic aperture radar imagery to assess hurricane- related flooding of coastal Louisiana. Int J Remote Sens 26(24):5359–5380

Klemas V (2014) Remote sensing of floods and flood-prone areas: an overview, J Coast Research 31(4):1005-1013

Knight AW, Tindall DR, Wilson BA (2009) A multitemporal multiple density slice method for wetland mapping across the state of Queensland, Australia, Int J Remote Sens 30:13, 3365-3392. DOI: 10.1080/01431160802562180

Kudahett C (2012) Flood mapping using synthetic aperture radar in the Kelani Ganga and the Bolgoda basins, Sri Lanka. Dissertation, University of Twente, The Netherlands

Lamovec P, Veljanovski T, Mikoš M, Oštir K (2013) Detecting flooded areas with machine learning techniques: case study of the selška sora river flash flood in September 2007. J Appl Remote Sens 0001, 7(1):073564-073564

Lillesand TM, Kiefer RW (2000) Remote Sensing and Image Interpretation, John Wiley & Sons, Inc., New York, N.Y, pp. 470-615

Long S, Fatoyinbo TE, Policelli F (2014) Flood extent mapping for Namibia using change detection and thresholding with SAR. Environ Res Let, 9:035002 (9pp)

Mason DC, Davenport IJ, Neal JC, Schumann GP, Bates PD (2012) Near real-time flood detection in urban and rural areas using high-resolution synthetic aperture radar images. IEEE Trans Geo Remote Sens 50(8): 3041–3052

Mirza MKM (2011) Climate change, flooding in South Asia and implications, Regional Environ Change 11 (Suppl I): S95-S107

Mosleh MK, Hassan QK (2014) Development of a remote sensing-based "boro" rice mapping system. Remote Sens 6:1938-1953

MPO (Master Plan Organization) (1987) Crop production limitations in Bangladesh. Technical Report No. 1. Master Plan Organization, Ministry of Irrigation, Water Development and Flood Control, Government of Bangladesh

Narvekar J, Prasanna KS (2006) Seasonal variability of the mixed layer in the central Bay of Bengal and associated changes in nutrients and chlorophyll. Deep-Sea Research Part I 53: 820–835

Nirupama, Simonović SP (2002) Role of Remote Sensing in Disaster. Institute of Catastrophic Loss Reduction (ICLR) London, ON, Canada. http://www.iclr.org/images/Role_of_Remote_Sensing_in_Disaster_Management.pdf Accessed 17 March 2015

NRCAN (Natural Resources Canada) (2016) Flood delineation and mapping. Web: http://www.nrcan.gc.ca/earth-sciences/geomatics/satellite-imagery-air-photos/satellite-imagery-products/educational-resources/9301 Accessed 15 June 2016

NWMP (National Water Management Plan) (2001) Water Resources Planning Organization, Ministry of Water Resources, Bangladesh, 26p.

Qi S, Brown DG, Tian Q, Jiang L, Zhao T, Bergen KM (2009) Inundation extent and flood frequency mapping using LANDSAT imagery and digital elevation model. GIScience Remote Sens 46(1):101–127. DOI: 10.2747/1548-1603.46.1.101

Rahman A, Khan K, Krakauer NY, Roytman L, Kogan F (2012) Use of remote sensing data for estimation of Aman rice yield. Int J Agric For 2(1): 101-107. http://dx.doi. org/10.5923/j.ijaf.20120201.16

Rashid H, Pramanik MAH (1993) Areal extent of the 1988 flood in Bangladesh: How much did the satellite imagery show? Nat Hazards 8(2):189-200

Senthilnath J, Shenoy HV, Rajendra R, Omkar SN, Mani V, Diwakar PG (2013) Integration of speckle de-noising and image segmentation using Synthetic Aperture Radar image for flood extent extraction. J Earth Syst Sci 122: 559. doi:10.1007/s12040-013-0305-z

Veiga V, Hassan QK, He J, Rahaman KR (2016) Exploring the potential of a Landsat-8 satellite image in mapping the 2013 flood extent over Calgary, Alberta. HazNet 8(1):24-28

Wu H, Adler RF, Tian Y, Huffman GJ, Li H, Wang J (2014) Rela-time global flood estimation using satellite-based preciptation and a coupled land surface and routing model, Water Resources Research 50:2693-2717

Yilmaz KK, Adler RF, Tian Y, Hong Y, Harold F (2010) Evaluation of a satellite-based global flood monitoring system, I J Remote Sens 31(14):3763-3782

List of Figures

Fig. 1 Location of the ground thruthing sites in the southwest shown as yellow dots on top of the Landsat TM images of 1997 (district boundaries are shown as black). Also blue diamond and green triangles indicated the location where we collected rainfall and water level data respectively.

Fig. 2 Characteristics of year 2000 rainfall during the early to late-monsoon periods for selected stations in southwest of Bangladesh.

Fig. 3 Setting of the year 2000 rainfall distribution during the monsoon period in comparison with the historical probable decadal rainfall (10, 50, and 90 % of the time) for selected stations in southwest of Bangladesh.

Fig. 4 The setting of year 2000 water level during the monsoon period in comparison with the historical probable decadal water levels (10, 50, and 90 % of the time) at selected key stations in southwest of Bangladesh.

Fig. 5 Illustration of no flooding in the southwest of Bangladesh during the peak flooding month of August using RADARSAT SAR images acquired on: (a) 26 Aug. 1998, and (b) 13 Aug. 2000.

Fig. 6 The open water flooding extent in blue color on 28 and 30 September 2000 extrated from RADARSAT ScanSAR images over portion of West Bengal in India and southwest of Bangladesh.

Fig. 7 SAR-derived multi-temporal backscattering singatures of the 7 classes in the southwest region of Bangladesh.

Fig. 8 Flood damage on *aman* crop in the southwest region (derived from the SWB images of August, September and October, 2000) of Bangladesh.

Fig. 9 Comparison of crop damage areas estimated from RADAR images and DAE of Bangladesh.

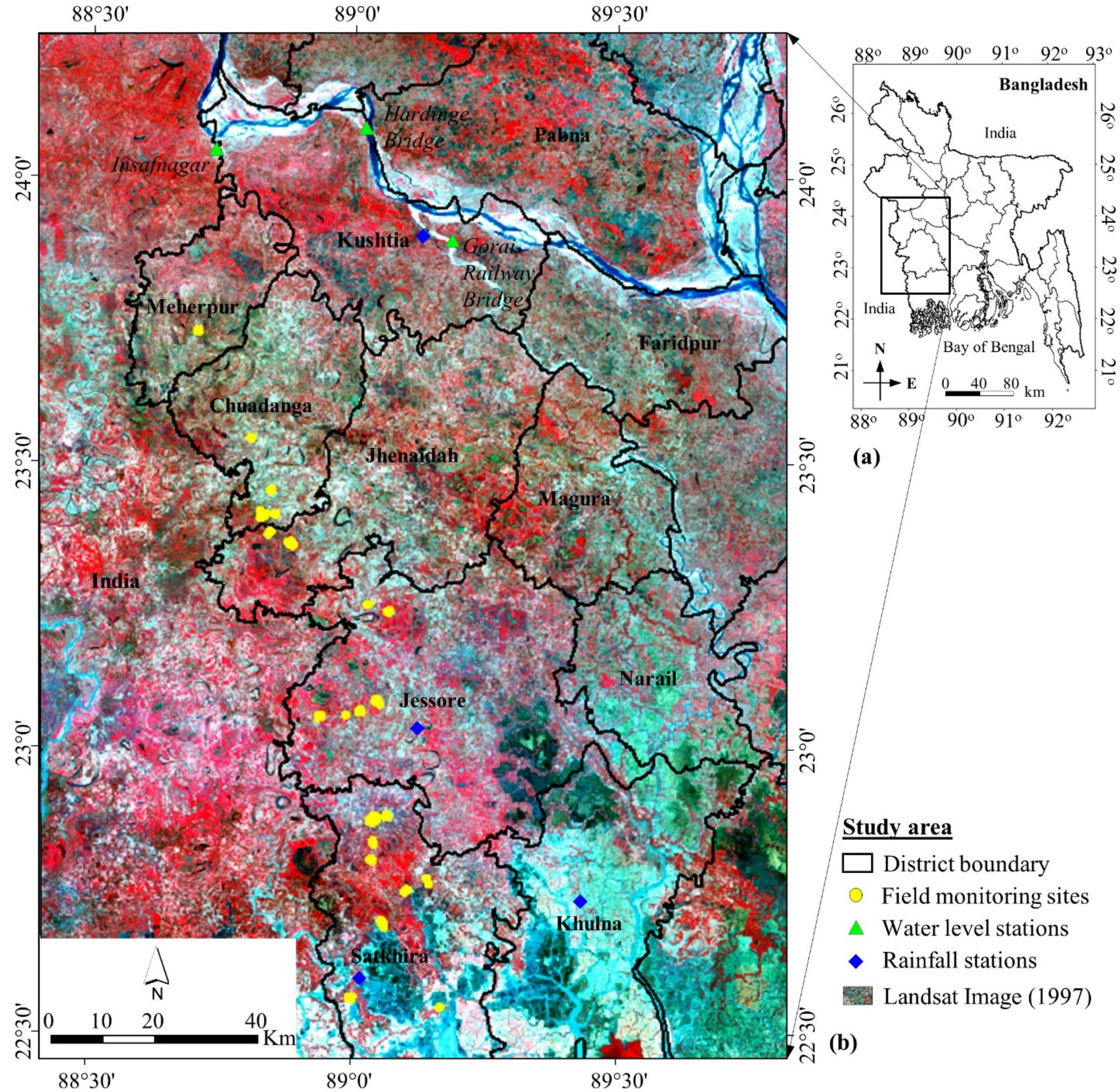
88°30'
89°0'
89°30'
24°0'
23°30'
23°0'
22°30'
Insafnagar
Hardinge Bridge
Pabna
Kushtia
Gorai Railway Bridge
Meherpur
Faridpur
Chuadanga
Jhenaidah
Magura
India
Narail
Jessore
Khulna
Satkhira
N
0 10 20 40 Km
88° 89° 90° 91° 92° 93°
Bangladesh
26° 25° 24° 23° 22° 21°
India
Bay of Bengal
E
0 40 80 km
(a)
Study area
District boundary
Field monitoring sites
Water level stations
Rainfall stations
Landsat Image (1997)
(b)

Fig. 1

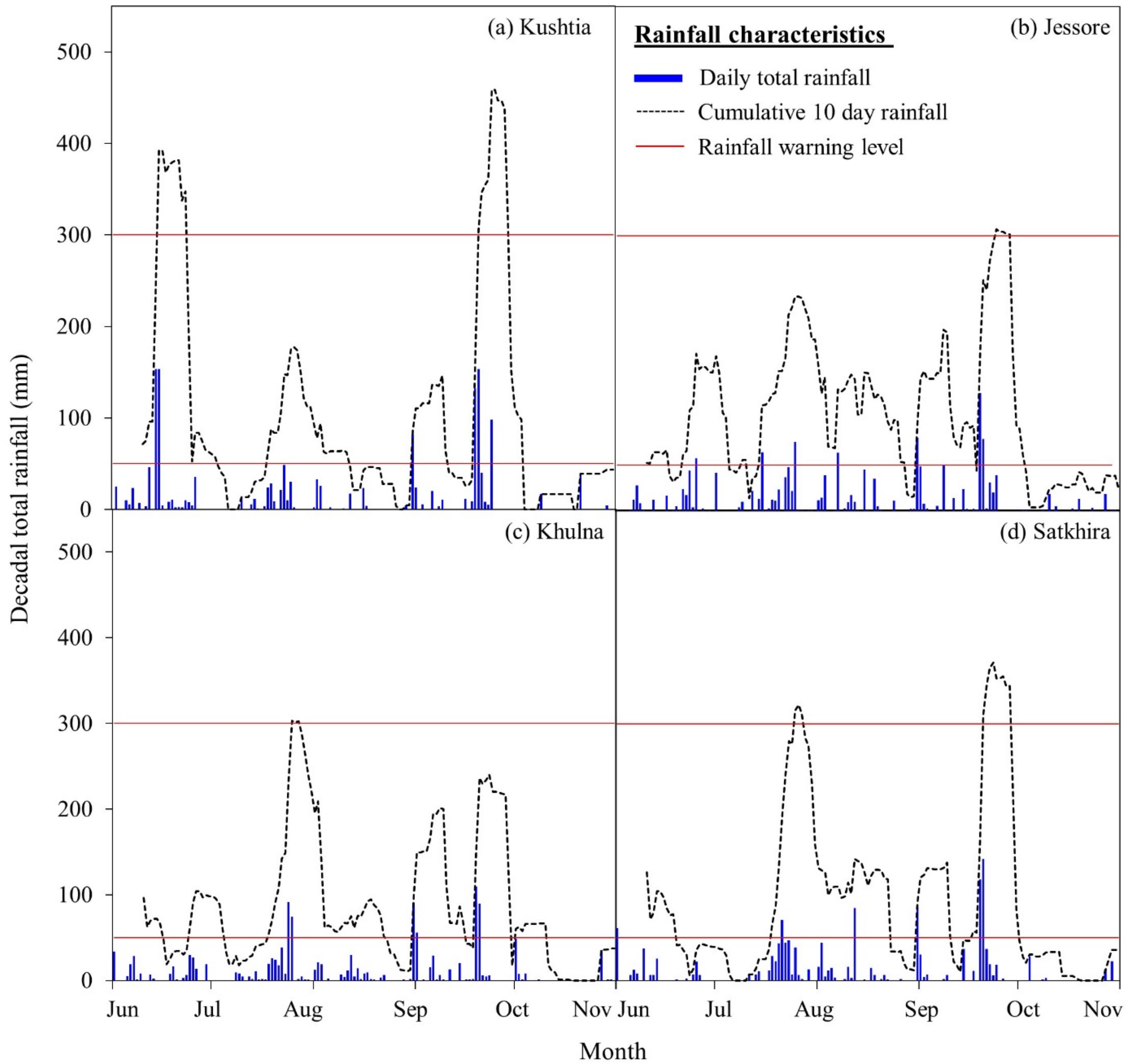
(a) Kushtia
(b) Jessore
(c) Khulna
(d) Satkhira
Rainfall characteristics
Daily total rainfall
Cumulative 10 day rainfall
Rainfall warning level
Decadal total rainfall (mm)
0
100
200
300
400
500
Jun
Jul
Aug
Sep
Oct
Nov
Month

Fig. 2

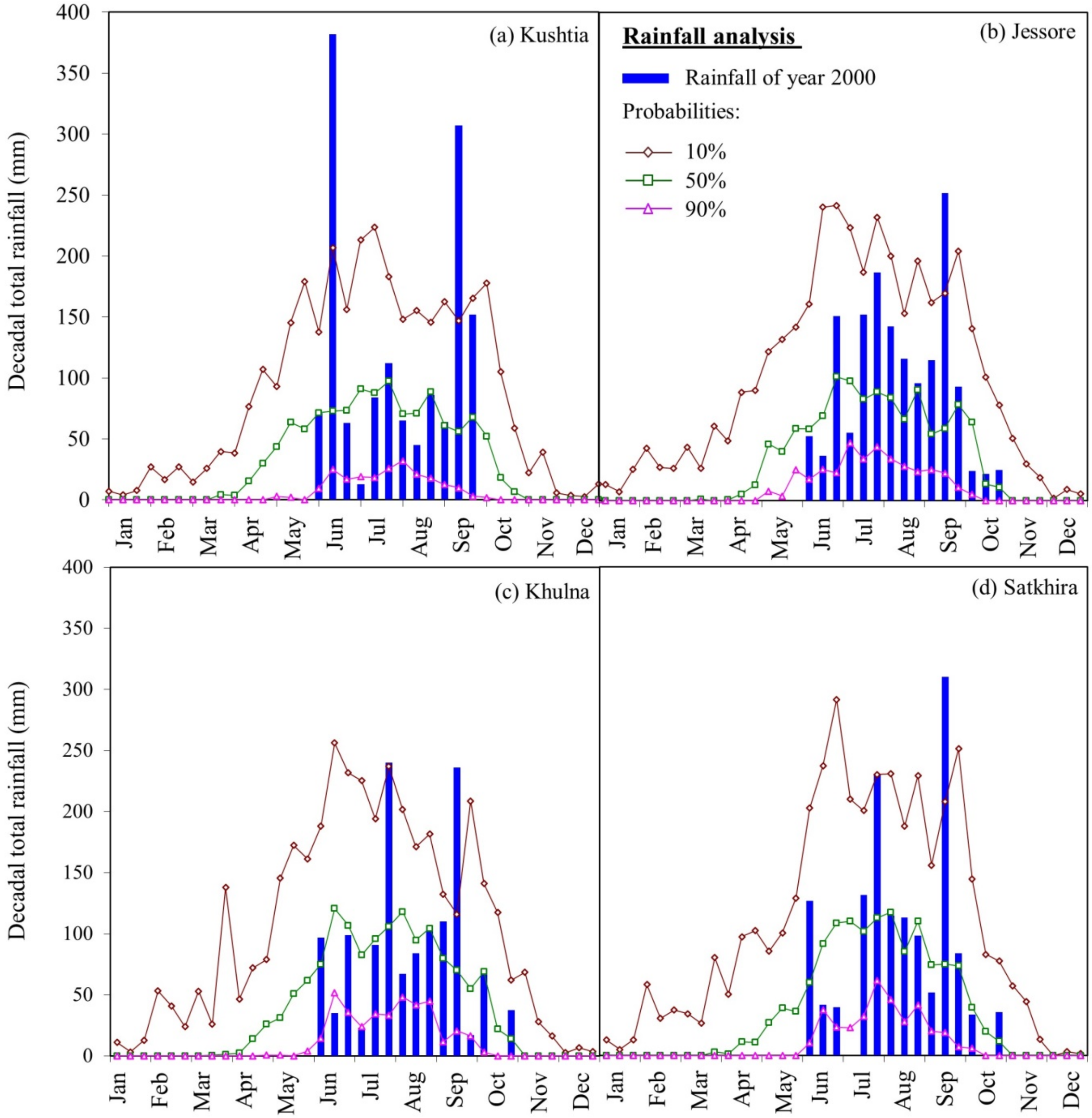
(a) Kushtia
(b) Jessore
(c) Khulna
(d) Satkhira
Rainfall analysis
Rainfall of year 2000
Probabilities:
10%
50%
90%
Decadal total rainfall (mm)
0
50
100
150
200
250
300
350
400
Jan
Feb
Mar
Apr
May
Jun
Jul
Aug
Sep
Oct
Nov
Dec

Fig. 3

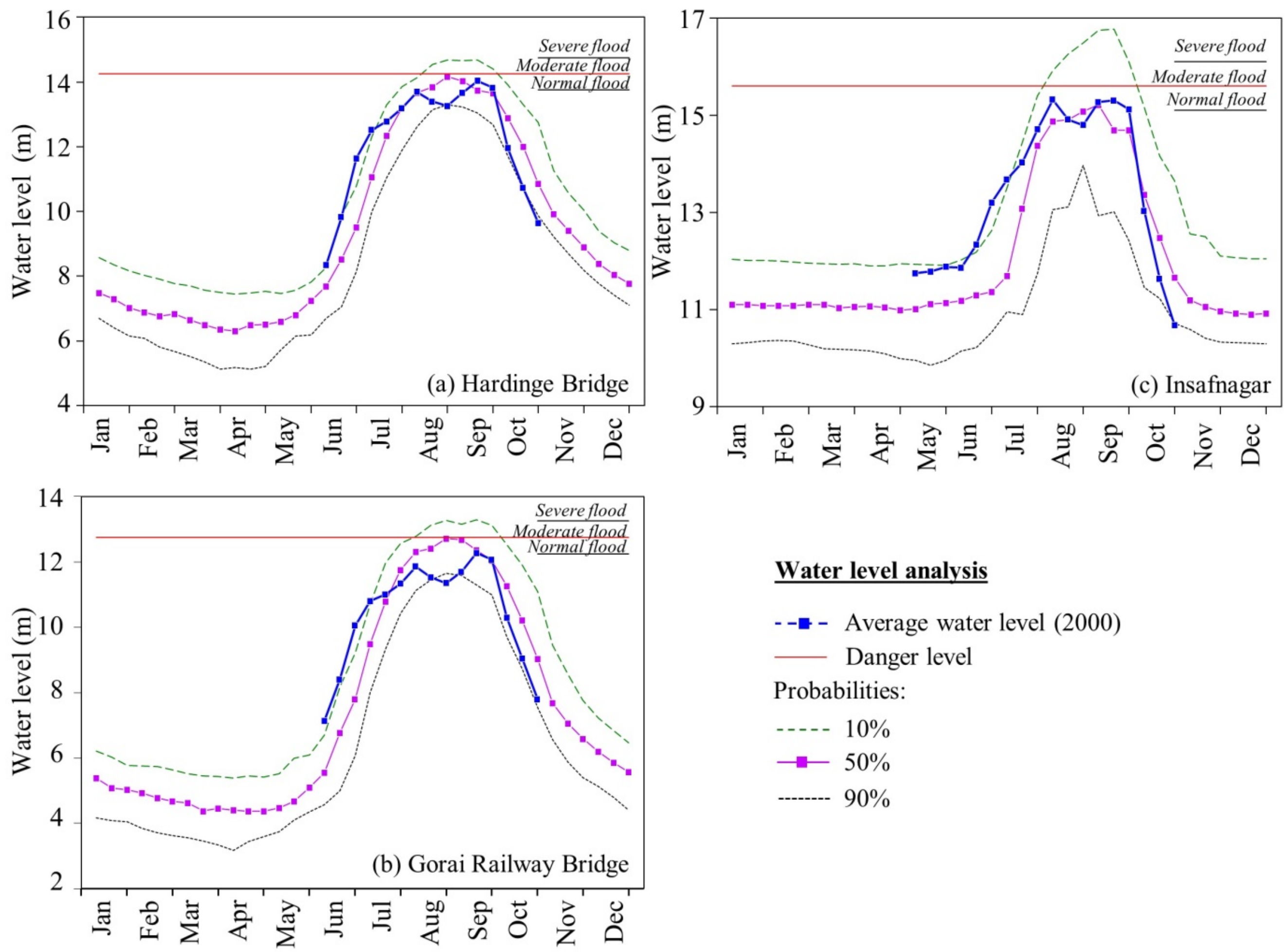
(a) Hardinge Bridge
(b) Gorai Railway Bridge
(c) Insafnagar
Water level (m)
Severe flood
Moderate flood
Normal flood
Jan
Feb
Mar
Apr
May
Jun
Jul
Aug
Sep
Oct
Nov
Dec
Water level analysis
Average water level (2000)
Danger level
Probabilities:
10%
50%
90%

Fig. 4

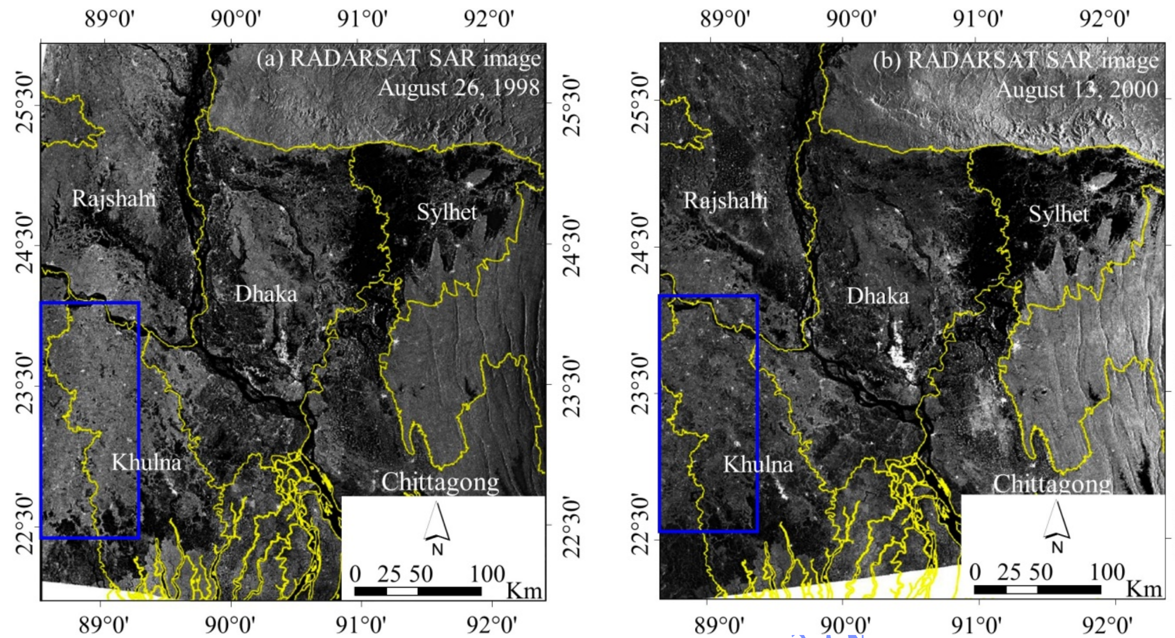

(a) RADARSAT SAR image
August 26, 1998
Rajshahi
Sylhet
Dhaka
Khulna
Chittagong
N
0 25 50 100
Km
89°0'
90°0'
91°0'
92°0'
25°30'
24°30'
23°30'
22°30'
(b) RADARSAT SAR image
August 13, 2000
Rajshahi
Sylhet
Dhaka
Khulna
Chittagong
N
0 25 50 100
Km

Fig. 5

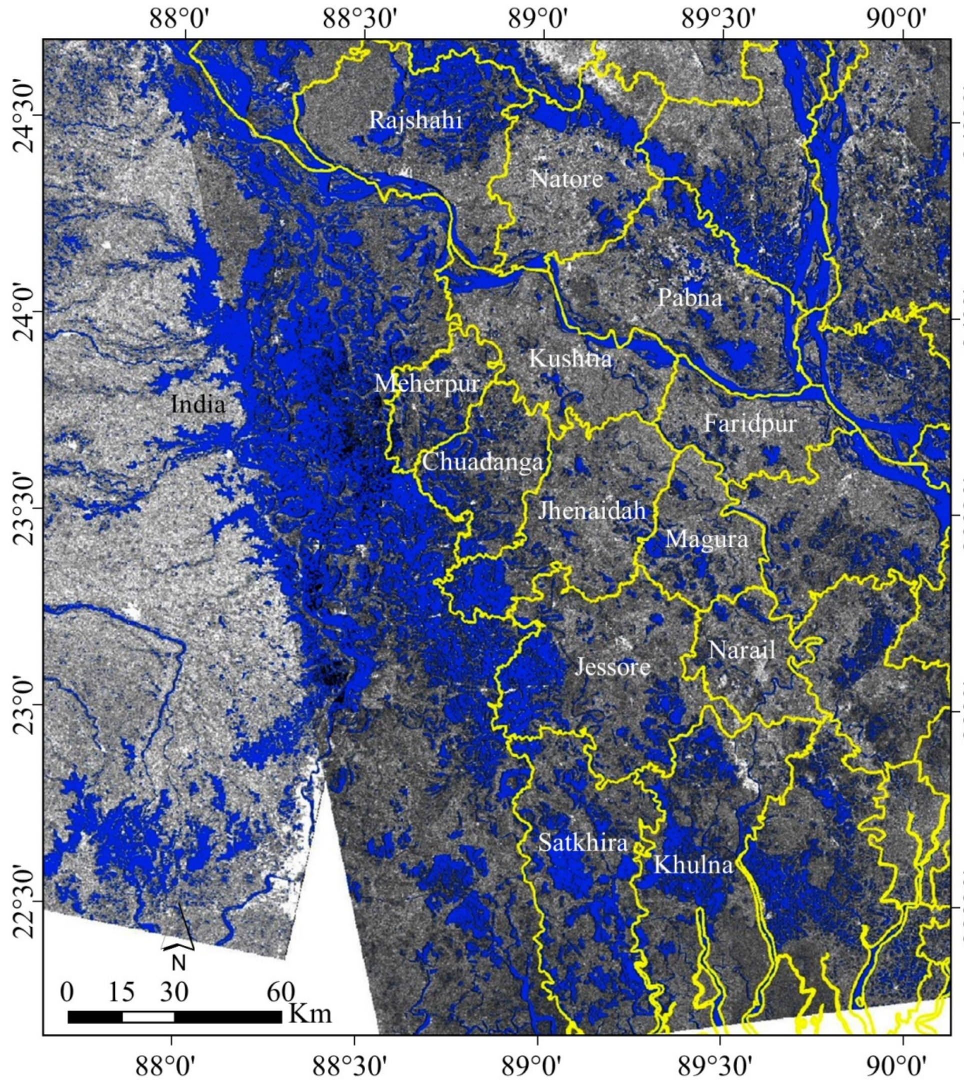

88°0'
88°30'
89°0'
89°30'
90°0'
24°30'
24°0'
23°30'
23°0'
22°30'
Rajshahi
Natore
Pabna
Kushtia
Meherpur
India
Faridpur
Chuadanga
Jhenaidah
Magura
Narail
Jessore
Satkhira
Khulna
N
0 15 30 60
Km

Fig. 6

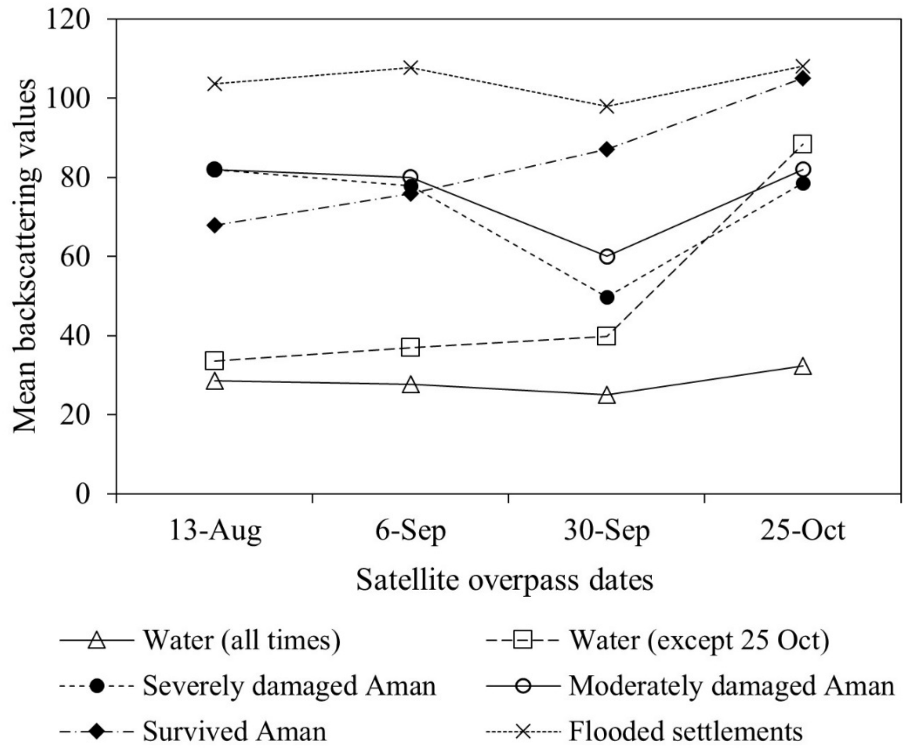

Mean backscattering values
120
100
80
60
40
20
0
13-Aug
6-Sep
30-Sep
25-Oct
Satellite overpass dates
Water (all times)
Water (except 25 Oct)
Severely damaged Aman
Moderately damaged Aman
Survived Aman
Flooded settlements

Fig. 7

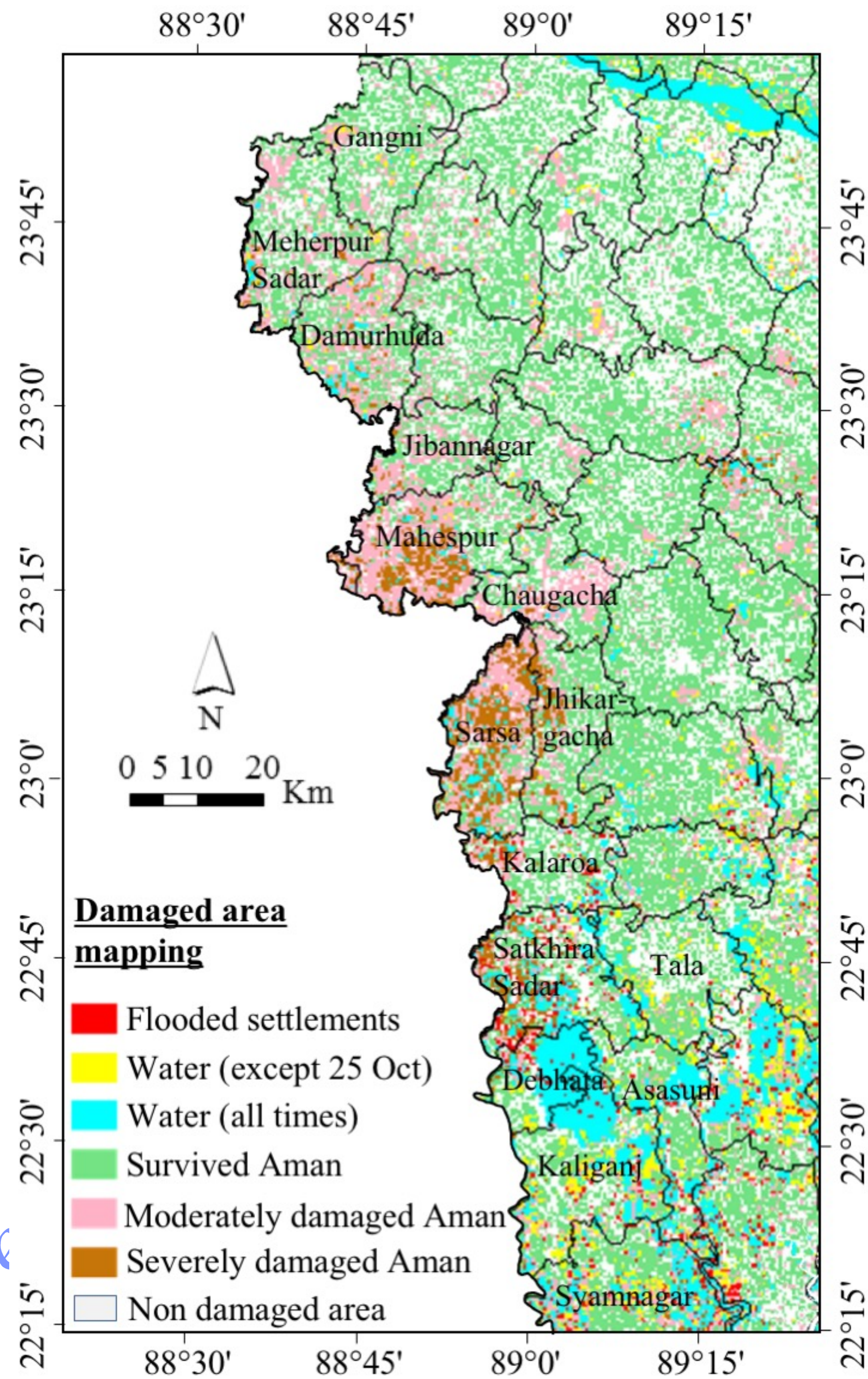
88°30'
88°45'
89°0'
89°15'
23°45'
23°30'
23°15'
23°0'
22°45'
22°30'
22°15'
Gangni
Meherpur
Sadar
Damurhuda
Jibannagar
Mahespur
Chaugacha
Jhikar-
gacha
Sarsa
Kalaroa
Satkhira
Sadar
Tala
Debhata
Asasuni
Kaliganj
Syamnagar
N
0 5 10 20
Km
Damaged area
mapping
Flooded settlements
Water (except 25 Oct)
Water (all times)
Survived Aman
Moderately damaged Aman
Severely damaged Aman
Non damaged area

Fig. 8

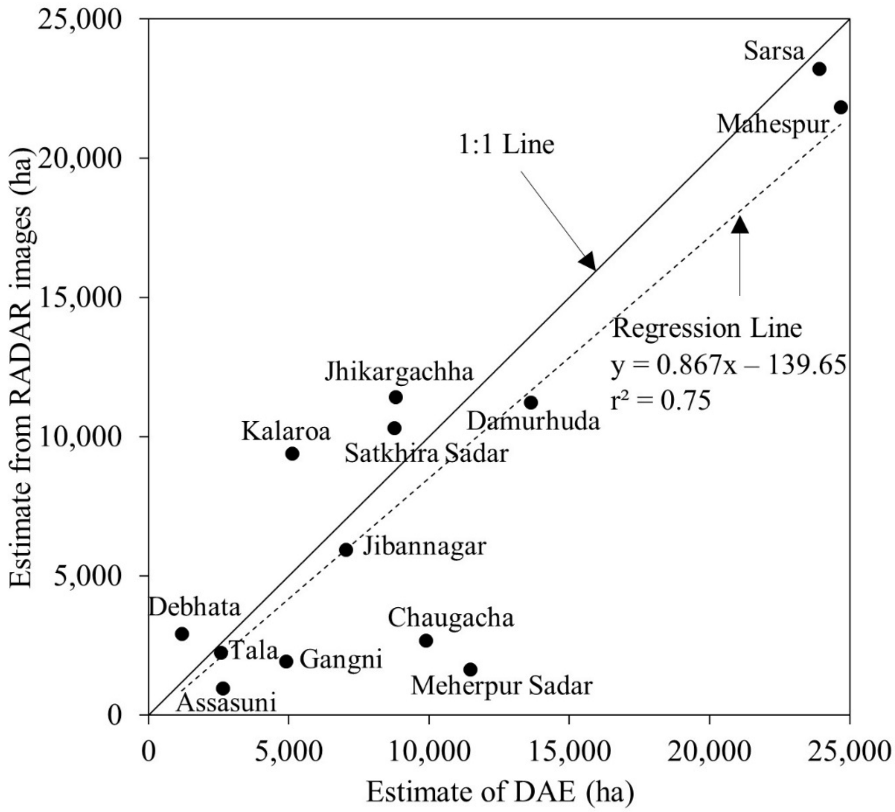
25,000
20,000
15,000
10,000
5,000
0
Estimate from RADAR images (ha)
0
5,000
10,000
15,000
20,000
25,000
Estimate of DAE (ha)
Sarsa
Mahespur
1:1 Line
Regression Line
y = 0.867x – 139.65
r² = 0.75
Jhikargachha
Kalaroa
Satkhira Sadar
Damurhuda
Jibannagar
Debhata
Tala
Gangni
Assasuni
Chaugacha
Meherpur Sadar

Fig. 9

List of Tables

Table 1 Description of RADARSAT SAR and IRS images used for damage assessment

Sensor	Path	Imaging date	Season
RADARSAT SAR, ScanSar Wide	Ascending	13 August, 2000	Monsoon
RADARSAT SAR, ScanSar Wide	Ascending	06 September, 2000	Monsoon
RADARSAT SAR, ScanSar Wide	Descending	28 September, 2000	Late Monsoon
RADARSAT SAR, ScanSar Wide	Ascending	30 September, 2000	Late Monsoon
IRS –1D LISS III	-	14 October, 2000	Late Monsoon
RADARSAT SAR, ScanSar Wide	Descending	25 October, 2000	Late Monsoon

Table 2 Variation of decadal total rainfall during year 2000 in comparison with the average year conditions (i.e., 50 %) for selected stations in southwest of Bangladesh

Station	June			July			August			September			October		
	1d	2d	3d	1d	2d	3d	1d	2d	3d	1d	2d	3d	1d	2d	3d
Jessore	-10	-47	49	-43	84	110	69	74	6	111	326	19	-62	59	126
Khulna	29	-71	-7	-72	-5	127	-43	-11	-1	38	237	-69	-3	-100	168
Kushtia	-1	424	-14	-86	-4	15	-8	-37	-3	5	450	124			
Satkhira	112	-55	-64	-100	29	105	-2	33	-11	-30	314	14	-15	-100	203

Blank cells represent missing data; 1d, 2d, and 3d – decades of the month;
Positive values indicate over average and negative values are below average conditions, respectively.

Table 3 Accuracy assessment of the SAR-based classified image using the ground truthing data

Ground truthing data (in hectare)	SAR-based classified image (in hectare): Water (all times)	Water (except 25 Oct)	Survived *Aman*	Severely damaged *Aman*	Moderately damaged *Aman*	Flooded settlements	*Row Total*	Producer's Accuracy	Omission Error
Water (all times)	**480.2**	24	0.25	0.2	0.2	0	*505*	0.95	0.05
Water (except 25 Oct)	49	**450.2**	18.2	0	3.7	0	*521*	0.86	0.14
Survived *Aman*	1.2	0.2	**552.2**	40.7	6.2	4.5	*605*	0.91	0.09
Severely damaged *Aman*	2.7	3.2	92.5	**393.2**	25	0.2	*517*	0.76	0.24
Moderately damaged *Aman*	20	5	103.7	32.5	**374.2**	0	*535*	0.70	0.30
Flooded settlements	0	1.2	75	0	26.2	**478.7**	*581*	0.82	0.18
Column Total	*553.2*	*483.8*	*841.8*	*466.6*	*435.5*	*483.4*	***3265.3***		
User's Accuracy	0.87	0.93	0.66	0.84	0.86	0.99			
Commission Error	0.13	0.07	0.34	0.16	0.14	0.01			